

## Journal Pre-proofs

Nanomaterials fusing with the skin: alpha-tocopherol phosphate delivery into the viable epidermis to protect against ultraviolet radiation damage

Mais M. Saleh, Arcadia Woods, Richard D. Harvey, Antony R. Young, Stuart A. Jones

PII: S0378-5173(20)30985-6  
DOI: <https://doi.org/10.1016/j.ijpharm.2020.120000>  
Reference: IJP 120000

To appear in: *International Journal of Pharmaceutics*

Received Date: 9 August 2020  
Revised Date: 16 October 2020  
Accepted Date: 17 October 2020



Please cite this article as: M.M. Saleh, A. Woods, R.D. Harvey, A.R. Young, S.A. Jones, Nanomaterials fusing with the skin: alpha-tocopherol phosphate delivery into the viable epidermis to protect against ultraviolet radiation damage, *International Journal of Pharmaceutics* (2020), doi: <https://doi.org/10.1016/j.ijpharm.2020.120000>

This is a PDF file of an article that has undergone enhancements after acceptance, such as the addition of a cover page and metadata, and formatting for readability, but it is not yet the definitive version of record. This version will undergo additional copyediting, typesetting and review before it is published in its final form, but we are providing this version to give early visibility of the article. Please note that, during the production process, errors may be discovered which could affect the content, and all legal disclaimers that apply to the journal pertain.

**Nanomaterials fusing with the skin: alpha-tocopherol phosphate delivery into the viable epidermis to protect against ultraviolet radiation damage**

Mais M. Saleh <sup>a</sup>, Arcadia Woods <sup>b</sup>, Richard D. Harvey <sup>c</sup>, Antony R. Young <sup>d</sup>, Stuart A. Jones <sup>b,\*</sup>

<sup>a</sup> Department of Pharmaceutics and Pharmaceutical Technology, School of Pharmacy, The University of Jordan, Amman 11942, Jordan

<sup>b</sup> Institute of Pharmaceutical Science, Faculty of Life Sciences & Medicine, Franklin-Wilkins Building, King's College London, 150 Stamford Street, London SE1 9NH, UK

<sup>c</sup> Department of Pharmaceutical Chemistry, University of Vienna, Althanstraße 14, Vienna, Austria

<sup>d</sup> St John's Institute of Dermatology, King's College London, Guy's Hospital, London, SE1 9RT, UK

\*Corresponding author. Dr. S. A. Jones. Tel: +44 (0)207 848 4843. Fax: +44 (0)207 848 4800.  
E-mail: [stuart.jones@kcl.ac.uk](mailto:stuart.jones@kcl.ac.uk)

## ABSTRACT

Vitamin E (alpha tocopherol,  $\alpha$ -T) is an important skin antioxidant, but its penetration into the viable epidermis, where it acts, is very limited. This study investigated if phosphorylating  $\alpha$ -tocopherol ( $\alpha$ -TP) to form a provitamin, improved its interactions with skin, its passage into the tissue, and thus its ability to protect the skin from ultraviolet radiation (UVR) damage. At pH 7.4, when the  $\alpha$ -TPO<sub>4</sub><sup>-1</sup> microspecies predominated in solution, dynamic light scattering measurements showed that  $\alpha$ -TP formed nanoaggregates with a median hydrodynamic diameter of 9 nm (CAC – 4.2 mM). At 9.0 when the  $\alpha$ -TPO<sub>4</sub><sup>-2</sup> microspecies predominated there was no aggregation. The passage of  $\alpha$ -TP nanoaggregates through regenerated cellulose membranes was significantly slower than the  $\alpha$ -TP monomers (at pH 9) suggesting that aggregation slowed diffusion. However, a lotion formulation containing the nanoaggregates delivered more  $\alpha$ -TP into the skin compared to the formulation containing the monomers. In addition, the nanosized  $\alpha$ -TP aggregates delivered 8-fold more active into the SC (252.2  $\mu$ g/cm<sup>2</sup> vs 29.5  $\mu$ g/cm<sup>2</sup>) and 4 fold more active into the epidermis (85.1  $\mu$ g/cm<sup>2</sup> vs 19  $\mu$ g/cm<sup>2</sup>, respectively,  $p < 0.05$ ) compared to  $\alpha$ -T. Langmuir subphase injection studies at pH 7.4 (surface pressure 10 mN m<sup>-1</sup>) showed that the  $\alpha$ -TP nanoaggregates more readily fused with the SC compared to the monomers. Membrane compression studies demonstrated that  $\alpha$ -TP fluidised the SC lipids. Together this SC fusion and fluidisation were proposed as the cause of the better  $\alpha$ -TP penetration into the SC and underlying epidermis and thus the enhanced potential of  $\alpha$ -TP to protect from UVR-induced skin damage compared to  $\alpha$ -T.

**KEYWORDS:** nanomaterials,  $\alpha$ -tocopherol phosphate, skin, stratum corneum, liposomes, skin interactions, delivery.

## Introduction

Molecules of a size of up to 500 g/mole, with a log P between 1-3, that are applied to outermost, dead layers of the skin, i.e., the *stratum corneum* (SC), can penetrate the underlying viable tissue by passive diffusion (1-3). However, the SC is a formidable barrier to xenobiotics that fall outside of this narrow range of physicochemical properties (4). The SC barrier properties are mainly conferred through its highly confluent layer of dead corneocytes cell ‘bricks’ embedded in a lipid (cholesterol, long-chain free fatty acid, and ceramide) ‘mortar’ (5,6).

Alpha-tocopherol ( $\alpha$ -T) is an important antioxidant that protects against ultraviolet radiation (UVR) induced oxidative stress. It inhibits UVR-induced DNA lesions even when applied after exposure (7-9). However, to obtain effective photoprotection, a significant amount of topically applied  $\alpha$ -T needs to reach the viable epidermis. In terms of physicochemical properties,  $\alpha$ -T ( $C_{29}H_{50}O_2$ , MW of 431.7 g/mole, log P 10) has two major limitations; firstly, it has poor chemical stability, due to sensitivity to light and oxygen, which reduces its shelf-life. Secondly,  $\alpha$ -T is very lipophilic, i.e., practically water-insoluble (calculated log P= 12, and  $pK_a$  above 10), thus it tends to localise in the SC, which reduces its penetration into the underlying viable skin layers (10). These limitations hinder the effectiveness of  $\alpha$ -T when applied to the skin.

Generating a more water-soluble  $\alpha$ -T derivative that is metabolised in the epidermis to form  $\alpha$ -T (i.e., a provitamin) is one approach that can be used to overcome the physicochemical limitations of  $\alpha$ -T. Such a derivative should increase  $\alpha$ -T stability, and its aqueous solubility to improve its skin deposition. The ester derivative of  $\alpha$ -T,  $\alpha$ -tocopherol phosphate ( $\alpha$ -TP), is more water-soluble and chemically stable compared to  $\alpha$ -T (11). However, the introduction of one phosphate into the  $\alpha$ -T generates an amphiphilic molecule, which renders it prone to aggregation. Previous work has shown that molecular aggregation can be detrimental to chemical penetration into the skin (12-13), but the effect of  $\alpha$ -TP aggregation on skin penetration has yet to be assessed.

The amphiphilic structure of  $\alpha$ -TP ( $C_{29}H_{49}O_5P$ , MW 508.7 g/mole, log P 10.78, log D 3.75) may play a fundamental role in modulating its interaction with SC lipids. The nonpolar region of  $\alpha$ -TP should be able to interact with the lipid hydrophobic core of SC whilst its polar phosphate group could engage in electrostatic interaction with skin lipid head groups, thus potentially enabling this molecule to reach skin layers that are inaccessible to the extremely

hydrophobic parent compound  $\alpha$ -T (14). In addition, an improved drug-vehicle interaction, produced by phosphate functionality of  $\alpha$ -TP, may enhance the solubilisation of the active in consumer product formulations compared to  $\alpha$ -T. However, there is a fine balance between the active-skin, active-vehicle, and active-active interactions that need to be achieved to achieve efficient skin penetration. Molecules that form aggregates cannot penetrate the skin as rapidly as single molecules and previous work has shown that size is sensitive to the type of vehicle in which they are applied and thus vehicle must be carefully optimised to generate a suitable topical product (12,15).

This study aimed to investigate how self-association and skin interactions of  $\alpha$ -tocopherol phosphate ( $\alpha$ -TP) influenced its deposition in the skin. To achieve this aim, the saturated solubility and tendency of  $\alpha$ -TP to form aggregates in aqueous vehicles were assessed. An ethanol/propylene glycol/Tris HCl buffer 20:20:60 % v/v/v was selected as a vehicle for  $\alpha$ -TP as it was able to solubilize the same amount of the active as the  $\alpha$ -TP commercial formulations (quasi pharmaceutical hair lotion formulations used in Japan) (11,16). Synthetic regenerated cellulose and silicone membranes were used to understand the effects of aggregation on diffusion and partitioning in model systems and this was anticipated to provide a mechanistic understanding of the systems before testing them in the skin. Porcine skin, an acceptable model of human skin, was used for the deposition studies, which were designed to understand how the applied  $\alpha$ -T and  $\alpha$ -TP from different formulations permeated into different skin layers (17,18). As the SC is the main barrier to chemical penetration into the skin, the interactions of  $\alpha$ -TP,  $\alpha$ -T, and a third provitamin  $\alpha$ -tocopherol acetate ( $\alpha$ -TA), with SC lipids were measured using an air/liquid interface monolayer model that employed a lipid barrier composed of an equimolar mixture of ceramide, cholesterol, and palmitic acid (Cer/Chol/PA) to mimic SC lipid lamellae (19). The ceramide that was used in this experiment belonged to the NS (non-hydroxy sphingosine) ceramide family with non-hydroxy fatty acid chains composed mainly of stearic acid (C18:0) and nervonic acid (C24:1) attached to a sphingosine head group through an amide bond (19). A lipid monolayer was used for the subphase injection studies that determined the adsorption kinetics of  $\alpha$ -TP,  $\alpha$ -T, and  $\alpha$ -TA from the subphase into the interfacial region occupied by the lipid monolayer. Compression isotherm analysis monitored changes in the lipid phase behaviour over a range of lipid-active compositions and surface pressures.

## Materials and methods

**Materials.**  $\alpha$ -TP (an all-racemic mixture of 8 isomers of dl- $\alpha$ -tocopherol phosphate, purity: 92.7%, cosmetic grade) was a gift from Shawa Denko (Tokyo, Japan).  $\alpha$ -T (type VI, ~ 40% purity, potency  $\geq 600$  mg d- $\alpha$ -tocopherol per g,  $\geq 1000$  IU/g),  $\alpha$ -tocopherol acetate ( $\alpha$ -TA) (Activity: 1306 IU/g, semisynthetic d- $\alpha$ -tocopherol acetate, synthesized from natural  $\alpha$ -tocopherol), bovine brain ceramide, cholesterol, palmitic acid, sodium chloride, dimethyl sulfoxide, propylene glycol, and trifluoroacetic acid were purchased from Sigma Aldrich (Dorset, UK). Hydrochloric acid was obtained from Fluka Chemicals (Gillingham, UK). High-performance liquid chromatography (HPLC) grade water, isopropanol, sodium hydroxide, chloroform, and tris base were sourced from Fisher Scientific (Loughborough, UK). Absolute ethanol was from VWR Chemicals (Leicestershire, UK). Miglyol 810 was from Cremer Oleo (Hamburg, Germany). Unless otherwise noted all the chemicals were analytical grade. Spectra/Por® cellulose ester (CE) dialysis membranes with molecular weight cut-offs (MWCO) of 0.5-1, 20, and 1000 kDa were sourced from Spectrum Labs (Netherlands, Europe).

**Solubility studies.** Saturated solutions of  $\alpha$ -TP were used to determine  $\alpha$ -TP solubility in a co-solvent composed of ethanol/propylene glycol/Tris HCl buffer 20:20:60 % v/v/v (n=3, 32°C, 24 h to reach equilibrium). The pH of the formulations was maintained at 3, 5.5, 7.4, and 9 using either 0.1 M HCl or 0.1 M NaOH. At equilibrium, the suspensions were transferred to 1.5 mL microcentrifuge tubes and centrifuged at 32°C for 15 min at 13,000 g and the supernatant was analysed using HPLC.

**Photon correlation spectroscopy (PCS).** The unattenuated derived count rate per second (kcps), which indicates the amount of light scattered by the sample, was used to analyse the extent of  $\alpha$ -TP aggregation in ethanol/propylene glycol/Tris HCl buffer 20:20:60 % v/v/v at both pH 7.4 and 9 at different concentrations (32.5 - 0.125 mM) (12, 13, 20). The solutions were analysed using a Zetasizer Nano-ZS (Malvern Instruments, UK) fitted with a 633 nm He-Ne laser. Detection of the light scattering signal was achieved at 137° backscattering angle at 32°C (to mimic the skin surface temperature) using the dispersant refractive index of 1.365, and viscosity 1.6122 mPa.s, the material refractive index was set at 1.59, the material absorbance at 0.01. Each measurement was comprised of 10-14 runs. Triplicates of each sample were assessed. The resultant kcps values were plotted against log drug concentration

and the critical aggregation constant (CAC) was determined by the intersection of two linear models applied to the data (12). The  $\alpha$ -TP nanoaggregate size was analysed at a concentration of 35 mM (above the CAC) using the same method. The aggregate size and polydispersity index (PDI, is the square of the standard deviation of the size distribution divided by the square of the mean) of  $\alpha$ -TP was monitored over time to assess short-term aggregate physical stability after incubation of 2% w/v TP at pH 7.4 for 0, 1, and 7 days in a water bath at 32°C.

**Atomic force microscopy.** Height images of the 3.5 mM  $\alpha$ -T and 0.9 mM and 6.3 mM  $\alpha$ -TP dispersed in the ethanol/propylene glycol/Tris HCl buffer 20:20:60 % v/v/v at pH 7.4 were obtained using an atomic force microscope (AFM; Bruker icon dimension, UK). Mica was chosen as a solid substrate on to which 2-3 drops of the test samples were placed; the samples were dried with nitrogen and then imaged. All images were obtained in tapping mode using high resonance frequency (HRF = 320 kHz) pyramidal cantilevers with uncoated Si<sub>3</sub>N<sub>4</sub> tips having force constants of 46 N/m in the air. Scan speeds were set at 0.9 Hz. Measurements were recorded using the NanoScope 1.50 AFM image analysis software (Bruker, USA) and were analysed using Gwyddion 2.45 software (freeware version; Czech Metrology Institute, Brno, Czech Republic).

**Chemical stability.** The chemical degradation rates of  $\alpha$ -TP (10, 20, and 100 µg/mL) when dispersed in ethanol/propylene glycol/Tris HCl buffer 20:20:60 % v/v/v were determined over a week at 32°C using high-performance liquid chromatography (HPLC, the method is described below).

**Synthetic membrane permeation studies.** A silicone membrane (thickness 0.12 mm, selected as it was the thinnest available from GBUK Healthcare, UK) and a cellulose ester (CE) dialysis membrane (three types: MWCO 0.5-1, 20 and 1000 kDa, Spectrum Labs, Breda, The Netherlands) were used for the artificial membrane transport studies. They were mounted in calibrated Franz diffusion cells with an average surface area of  $2.22 \pm 0.11$  cm<sup>2</sup>, an average receptor compartment volume of  $8.93 \pm 0.35$  mL, loaded with a 13 mm magnetic stirrer in the receptor chamber to avoid the build-up of the drug at the lower membrane interface. Miglyol oil was also loaded into the receiver chamber, the cells were allowed to equilibrate at 37°C for 60 min, they were inverted to check the membrane integrity and any leaking cells were resealed (12). For the silicone membrane studies, 1 mL, i.e., an infinite dose, of  $\alpha$ -T oil used as supplied,  $\alpha$ -TA oil used as supplied, and  $\alpha$ -TP, which was saturated in Miglyol fluid (1.7 mg/mL), was



applied to the apical surface of the membrane. The donor chamber was covered with aluminum foil and parafilm, to protect from light and prevent evaporation of the solution during the study. Aliquots of 1 ml were withdrawn using a plastic syringe, from the sampling arm of the Franz cell receiver compartment, at 0.5, 1, 2, 3, 4, 5, and 24 h and replaced immediately with an equal volume of the pre-warmed receiver fluid to keep the liquid volume in the receiver compartment constant. The samples were dissolved in the mobile phase then transferred to HPLC vials to assay  $\alpha$ -TA,  $\alpha$ -T, and  $\alpha$ -TP content at each time point. The cellulose ester membrane studies characterised the diffusion of  $\alpha$ -TP at both pH 7.4 and pH 9.0 from 1 mL of 90% saturated solutions across the membrane using Franz diffusion cells. The  $\alpha$ -TP was dissolved in the ethanol/propylene glycol/Tris 20:20:60 % v/v/v vehicle and the same co-solvent was used as the donor solution to prevent the effects of solvent back diffusion. The Franz cell receiver compartment was sampled at 1, 2, 3, 4, 5, 6, and 24 h. Three different cellulose molecular weight cut-offs, i.e., 0.5-1 kDa, 20 kDa, and 1000 kDa were compared, each with an n=5. The diffusion of the actives through porous membranes with different size pores was anticipated to provide a richer understanding of how the different sizes of the  $\alpha$ -TP monomers and  $\alpha$ -TP aggregates altered their diffusion.

For both silicone and cellulose membrane studies, cumulative amounts of the drug ( $\mu$ g) penetrating per unit surface area of the membrane ( $\text{cm}^2$ ) were corrected for sample removal and plotted against time (h). Steady-state flux ( $J_{ss}$ ) was calculated from the slope of the linear portion of the curve ( $R^2 > 0.99$ ), using at least 4 points with values above the assay limit of quantification (LOQ). All data were checked to ensure sink conditions, i.e., sample donor solution did not fall  $< 90\%$  of its initial concentration and the receiver solution did not accept permeant concentrations that exceed  $> 10\%$  of the total permeant saturated concentration in the receiver fluid. All the reported data complied with these conditions.

**Skin deposition studies.** Skin deposition of  $\alpha$ -T pure oil,  $\alpha$ -TP lotions (pH 7.4 and pH 9), and a commercial  $\alpha$ -TP lotion (pH 6.8) (See Fig.S1 for commercial formulation details) were assessed. The porcine skin studies used white adult pig ears sourced from a local abattoir (Ginger Pig, London, UK). These ears were cleaned with deionized water and residual hair was trimmed. Tissue was either used immediately or stored at  $-20^\circ\text{C}$  for a maximum of 3 days and after which it was thawed out carefully before use. The skin was carefully pulled from the ear cartilage and subcutaneous fat was removed by forceps and scalpel. Each study used several



different ears. Tissue thickness was  $1.67 \pm 0.72$  mm as measured by a micrometer (Starrett Company Ltd., Jedburgh, Scotland). The tissue was mounted in the Franz cells as described previously, equilibrated, checked and the test chemicals applied (matched in terms of thermodynamic activity ( $\alpha=1$ )). The volume of topically applied test systems (pure  $\alpha$ -T pure oil, and  $\alpha$ -TP saturated solutions) was varied to give a dose of  $8.7 \pm 0.9$  (range 7.5-9.2) mg/cm<sup>2</sup>. At 3 h (preliminary studies suggested steady-state permeation was achieved) samples were taken from the receiver fluid, the Franz cells were dismantled and the donor compartment was washed with methanol (the washings were retained for analysis). The skin was removed and cleaned with cotton buds (later extracted with methanol and retained for analysis) and mounted on a corkboard. The SC was removed by tape stripping (ca. 22 strips until the skin was translucent) using adhesive tape (Scotch 845 book tape, 3M, Bracknell, UK) (21), and the first two strips were considered as part of the applied formulation and hence its removal was part of the formulation wash off (22). The tape strips were applied sequentially covered using a 500 mg weight for 10 s and then removed. Once removed, the strips were collected together and the active was extracted by immersion in 100% MeOH (validated by preliminary work). The test agents were extracted from the epidermis and dermis by separating the epidermis from the dermis using a scalpel as previously reported (23). Both the epidermis and dermis were homogenized using 100% MeOH and left in contact with the extraction solution for 24 h. Samples were then centrifuged at 17000 rpm (Biofuge, Heraeus, Germany) for 15 min. The skin surface wash off solution, the SC extraction fluid, the epidermis, and dermis supernatants were analysed using HPLC. The total recovery efficacy was  $98.2 \pm 2.2\%$ .

**Quantification method of  $\alpha$ -TP.**  $\alpha$ -TP quantification was performed using reversed-phase HPLC. The set up consisted of a 717 plus auto-sampler (Waters, Elstree, UK), a photodiode array UV detector, and a quaternary pump (Spectra Physics, UK). The detection wavelengths for  $\alpha$ -TP,  $\alpha$ -T, and  $\alpha$ -TA were 287, 290, and 284 nm, respectively. The mobile phase comprised isopropanol/water (85:15 v/v) and 0.1 % trifluoroacetic acid (TFA) set at a flow rate of 1 mL min<sup>-1</sup> for  $\alpha$ -TP and 1.2 mL min<sup>-1</sup> for  $\alpha$ -T and  $\alpha$ -TA to optimise the retention time.  $\alpha$ -TP was separated using a C18 stationary phase (Phenomenex 5  $\mu$ m, 250 x 4.60 mm) at room temperature with a 50  $\mu$ L injection volume. For the skin permeation studies that employed Miglyol oil as the receiver fluid the ratio of the mobile phase was modified to isopropanol/water (90:10, v/v) to enhance the solubility of Miglyol oil in the mobile phase and the flow rate was set at 1 mL min<sup>-1</sup>. All the other parameters were kept the same. The assay precision was <

2.18%, the calibration linearity was  $> 0.9999$ , the limit of detection was  $1.13 \mu\text{g/mL}$  and the limit of quantification was  $3.42 \mu\text{g/mL}$ .

**Monolayer subphase injection studies.** A 50 mm diameter perfluoroalkoxy alkane (PFA) Petri dish (Saint-Gobain, Poestenkill, NY, USA) with a maximum volume of 20 mL was placed on a stirring plate (Whatman stirrer, WC-303), filled with tris-HCl buffer (0.1 M, at pH 7.4), with a Wilhelmy plate (Whatman, grade 1, chromatographic paper) connected to a calibrated NIMA PS4 (0-240 mN/m range, 0.1 mN/m resolution) pressure microbalance (NIMA technology equipment Ltd, Coventry, England) used to monitor surface pressure (Nima TR516 software). The Petri dish was used to perform a constant area assay using a skin SC lipid monolayer model, which consisted of equimolar mixtures (1:1:1) of ceramide, cholesterol, and palmitic acid (Cer/Chol/PA). This mixture was used to mimic SC intercellular lipids at the air/liquid interface, as described previously (19). The SC lipid monolayer film was produced using 5.1 mg ceramide, 4 mg cholesterol, and 3 mg palmitic acid dissolved in 5 mL chloroform (a 2.4 mg/mL lipid mixture, dissolved in chloroform). In this assay, two drops of lipid solution were spread on the buffered subphase and left to stand for at least 15 min. After the solvent had evaporated and the lipid monolayer had equilibrated a stable surface pressure was obtained ( $\leq 0.2 \text{ mN/m}$  over 2 min). A 100  $\mu\text{L}$  aliquot of  $\alpha$ -TP (concentration of 1, 2, and 12 mM) in the vehicle (ethanol/propylene glycol/Tris HCl buffer 20:20:60 % v/v/v) was injected into the subphase below the SC lipid monolayer film and the surface pressure was monitored over time at a constant surface area. The experiment was repeated using 2.3 mM (1 mg/mL)  $\alpha$ -T in the same vehicle at pH 7.4 or DMSO and using 2.1 mM (1 mg/mL)  $\alpha$ -TA in DMSO. The test compound-lipid interactions were measured by a change in surface pressure over time. The adsorption profiles (the increase in the surface pressure at the time of drug injection) obtained were fitted using OriginPro software by a nonlinear curve fit (Hill) model according to equation 1 to estimate the three parameters, the maximum obtained surface pressure ( $\Delta\Pi_{\text{max}}$ ), the time to reach 50% of maximum surface pressure ( $t_{50}^h$ ), and the Hill slope ( $h$ ).

$$y = \frac{\Delta\Pi_{\text{max}}x^h}{t_{50}^h + x^h} \quad (1)$$

**Compression isotherm analysis.** A Langmuir trough (Model 612D, NIMA Langmuir-Blodgett (LB) NIMA technology equipment, Ltd, Coventry, England) (area  $600 \text{ cm}^2$ ) was used to acquire surface pressure-area ( $\Pi$  -A) isotherms. Model SC lipid monolayers were deposited

onto a 150 mM NaCl subphase (300 mL), from a 1 mg/mL solution in chloroform. In total, 40  $\mu$ L of SC lipid solution or SC lipid/active mixtures containing 10%, 30%, or 60% (v/v)  $\alpha$ -TP was spread at the air/liquid interface and left for 15 min to allow solvent evaporation. Following evaporation, the monolayers were compressed with a constant slow barrier speed of 6 cm<sup>2</sup>.min<sup>-1</sup> until their collapse point was reached. Films composed of 100%  $\alpha$ -TP, 100%  $\alpha$ -T, and 100%  $\alpha$ -TA were used as controls.

The interaction between the SC lipids and the  $\alpha$ -TP was further evaluated with mean molecular area (MMA) plots. The MMA of five different SC lipid/ $\alpha$ -TP mixtures were plotted as a function of  $\alpha$ -TP percentage at nine surface pressures to provide a measure of miscibility between the SC lipids and the  $\alpha$ -TP. MMAs were calculated according to the additivity rule, as shown in equation 2.

$$A_{12} = X_1A_1 + X_2A_2 \quad (2)$$

$A_1$  and  $A_2$  represent MMAs for the SC lipids (assumed to be an ideal mixture) and the test agent, e.g.,  $\alpha$ -TP, respectively, under the same surface pressures while  $X_1$  and  $X_2$  are the fractions of each component in the mixture. If two components are ideally mixed or phase-separated, the MMA of their mixtures follows the additivity rule. Repulsive or attractive interactions in binary lipid mixtures can be assessed respectively by positive or negative deviation from the additivity rule.

The compressibility of a monolayer can be used to characterise its phase state (24-26). The compressibility ( $C_s$ ) of a monolayer at any area,  $A$ , is defined according to equation 3. However, for more precise measurement, the reciprocal of  $C_s$  is used to characterise the properties of the surface film and is called the surface compressibility modulus ( $k^s$ , or  $C_s^{-1}$ ), which is defined according to equation 4. The compressibility properties can be determined from the slope of a  $\pi$ - $A$  isotherm at specific surface pressures (27).

$$C_s = -\frac{1}{A} \left( \frac{\delta A}{\delta \pi} \right)_T \quad (3)$$

$$K^s = -A \left( \frac{\delta \pi}{\delta A} \right)_T \quad (4)$$

Where  $\delta A$  refer to a change in the area ( $\text{\AA}^2/\text{molecule}$ ),  $\delta\pi$  refers to a change in interfacial surface pressure value ( $\text{mN m}^{-1}$ ), and  $T$  indicates this is true for a specific temperature. The phase state of monolayer are classified by  $K^s$  ranges into liquid expanded phase (12.5-50  $\text{mN/m}$ ), the intermediate phase between liquid expanded to liquid condensed (higher than 50 below 100  $\text{mN/m}$ ) liquid condensed phase (100-250  $\text{mN/m}$ ), and solid-state (1000-2000  $\text{mN/m}$ ) (24).

**Statistical analysis.** All the values were expressed as their mean  $\pm$  standard deviation (SD). The homogeneity of variance (Levene's test) and the normality (Shapiro-Wilk test) of all data sample groups was assessed before statistical analysis. The critical aggregate concentration (CAC) analysis was performed using OriginPro software (OriginPro version 8.6, OriginLab Corporation, US). The statistical analysis was performed using the statistical package of social sciences, SPSS version 17 (IBM Corp., USA) with a significance level of 0.05. Two-group comparison of the mean values was performed using Student's independent t-test for data with equal variance or Mann-Whitney's test for data with non-equal variance. A one-way analysis of variance (ANOVA) test was employed for normally distributed data with more than two groups and a non-parametric Kruskal-Wallis test was used for non-normally distributed data with more than 2 groups. *Post hoc* comparisons of the means of individual groups were performed when appropriate using Tukey's test or Dunnett's test for equal variance normally distributed data, whereas or Games Howell test for unequal variance non-Gaussian distributed data. Data were presented using Prism software (GraphPad Prism, version 5.02, December 2008).

## Results

**Solubility studies.** In order to understand how the  $\alpha$ -TP ionisation influenced the compound solubility saturated solutions were prepared and the maximum solubility was determined at 4 different pH's in an ethanol/propylene glycol/Tris HCl buffer 20:20:60 % v/v/v co-solvent. The solubility of  $\alpha$ -TP in the co-solvent at 32°C, was  $0.21 \pm 0.01$  mg/mL,  $0.48 \pm 0.1$  mg/mL,  $20.56 \pm 1.39$  mg/mL and  $36.45 \pm 2.27$  mg/mL at pH 3, 5.5, 7.4 and 9, respectively. The solubility significantly increased when increasing the pH above 6 ( $p_{ka_2}$ ) ( $p < 0.001$  at pH 7.4 and  $p < 0.01$  at pH 9, Games-Howell test, multiple comparisons one-way ANOVA, Fig. 1).

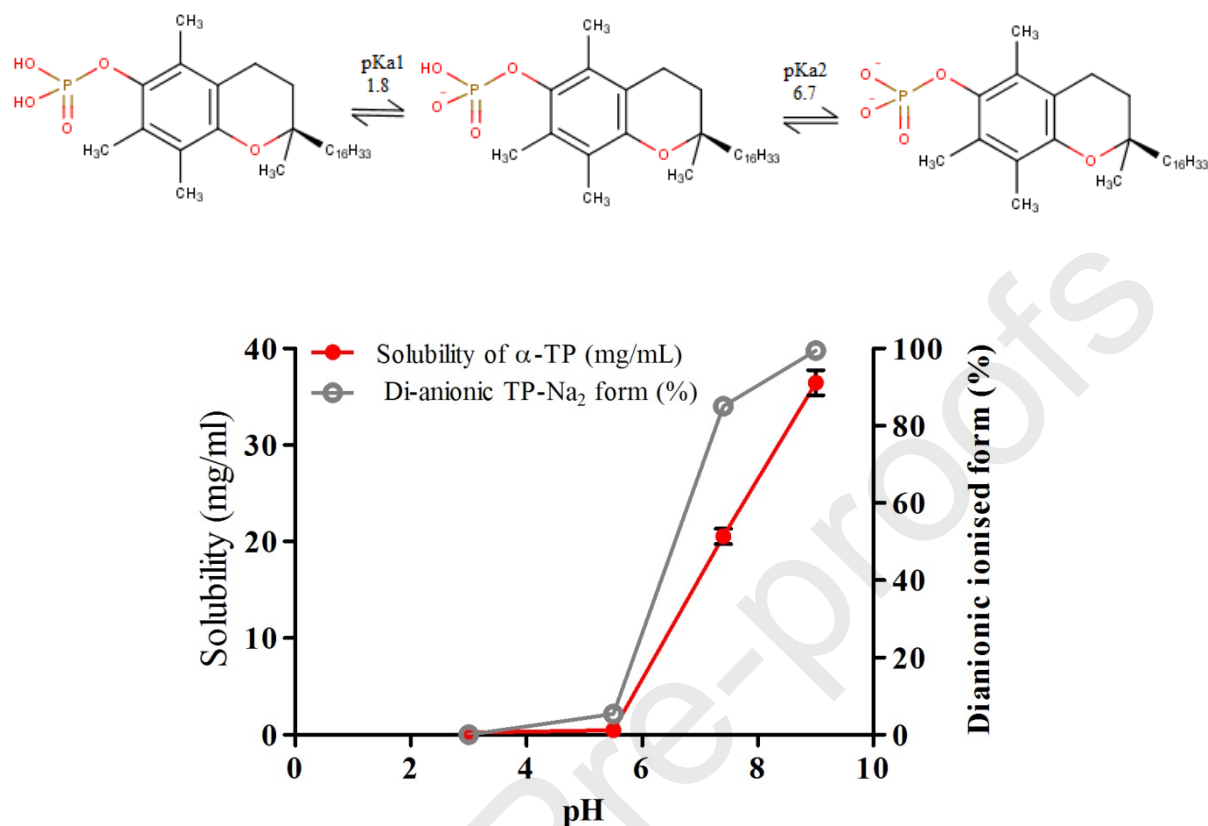


Fig.1: The aqueous solubility of  $\alpha$ -TP in 20:20:60 % v/v/v ethanol: propylene glycol: Tris cosolvent at different pHs at 32 °C. Data represent the mean  $\pm$  SD (n=3). The image shows the conversion of the  $\alpha$ -tocopherol phosphate into a mono then dianion.

**Aggregation of  $\alpha$ -TP.**  $\alpha$ -TP formed aggregates at a CAC of 4.19 mM in the 20:20:60 % (v/v/v) ethanol/propylene glycol/Tris co-solvent at 7.4 (Fig. 2). No trend in the light scattering data was observed when the dispersion vehicle was at pH 9.0, which suggested that no aggregation occurred over the concentration range tested. The aggregation of  $\alpha$ -T could not be measured accurately due to its limited solubility in the vehicle.

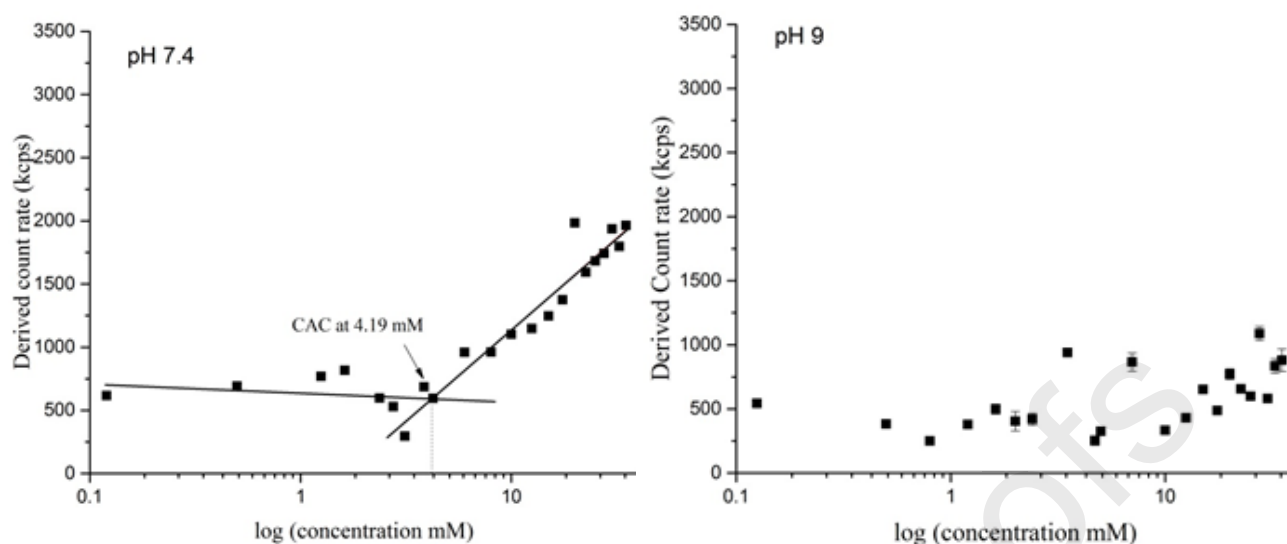


Fig. 2: A plot of unattenuated light scattering derived count rate vs log concentration of  $\alpha$ -TP at pH 7.4 (a) and pH 9 (b) (32°C). CAC refers to critical aggregation concentration, note that at pH 9 the data indicated that there was no aggregation. Data represent the mean  $\pm$  SD (n=3).

**Aggregate size and physical stability.** The AFM images showed that at a 0.9 mM concentration  $\alpha$ -TP formed circular aggregates with diameters of  $51.67 \pm 4.51$  nm and height of  $17 \pm 0.5$  nm (range 16-17 nm) (n=3) (Fig.3 a,b) and at higher concentration (6.3 mM) it formed rods with a width of  $306.7 \pm 35.1$  nm and a length of  $571.3 \pm 28.9$  nm and a height of  $9.5 \pm 0.5$  nm (range 9-10 nm) (Fig S2). The AFM derived diameter of the  $\alpha$ -T aggregates at 3.5 mM was  $373.30 \pm 28.87$  nm (n=3) and the height was  $52.0 \pm 8.0$  nm (range 46-60 nm) (Fig.3 c, d). Note it was not possible to obtain images at equivalent  $\alpha$ -TP and  $\alpha$ -T concentrations due to differences in their propensity to aggregate.

The DLS derived size of the  $\alpha$ -TP aggregates using a concentration of 35 mM  $\alpha$ -TP was  $9.36 \pm 1.59$  nm (n=3) (Fig. 4.a). The DLS size of the  $\alpha$ -T aggregates using a concentration of 1 mM was  $205.15 \pm 21.28$  nm (n=3) (Fig. 4.b). The  $\alpha$ -TP aggregate hydrodynamic size and PDI showed no major changes (See table 1 in the supporting information) in the 20:20:60 % (v/v/v) ethanol/propylene glycol/Tris co-solvent over 7 days storage at 32°C.

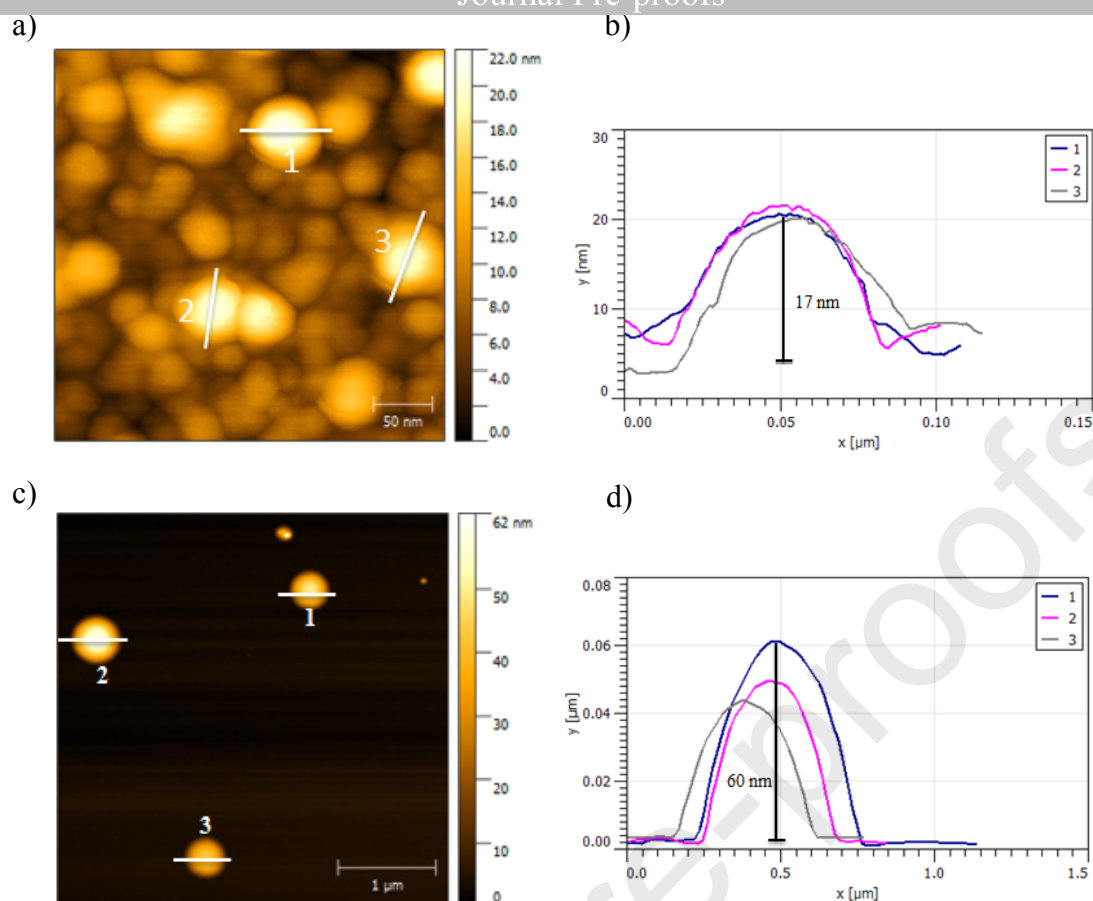


Fig.3: Atomic force microscopy tapping height images (left), cross-section profile (right) of 0.9 mM  $\alpha$ -TP (a,b), 3.5 mM  $\alpha$ -T (c,d).

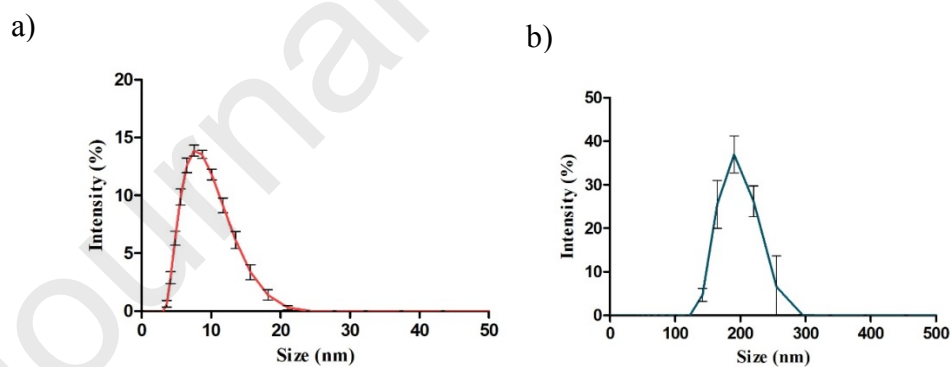


Fig.4: Hydrodynamic size of 35 mM  $\alpha$ -TP (a) and 1 mM  $\alpha$ -T (b) using dynamic light scattering. Data represent mean  $\pm$  SD ( $n=3$ ).

**Chemical stability.** A 100  $\mu$ g/mL sample of  $\alpha$ -TP lost 3.3% of its initial concentration over a week when dissolved in the 20:20:60 % (v/v/v) ethanol/propylene glycol/Tris co-solvent.



However, at 20 µg/mL and 10 µg/mL, it lost 7.6% and 12.8% of its initial concentration (See table S2).

**Artificial membrane permeation studies.** To understand how the diffusion of the molecule changed when varying ester groups were added to the  $\alpha$ -T, the ability of different forms of the molecule to pass through a confluent silicone synthetic membranes was assessed. The flux of  $\alpha$ -TA through silicone membrane was statistically higher than  $\alpha$ -T ( $3,278.87 \pm 223.48$  vs  $1,513.03 \pm 97.14$  µg.cm<sup>-2</sup>.h<sup>-1</sup>,  $p < 0.01$ , Mann-Whitney's test) (See Fig. S3). The 24 h cumulative amount of  $\alpha$ -TA that penetrated the membrane was also significantly higher than  $\alpha$ -T ( $43,465.27 \pm 8,170.76$  vs  $20,857.16 \pm 2,703.65$  µg.cm<sup>-2</sup>,  $p < 0.05$ , Mann-Whitney's test).  $\alpha$ -TP could not be detected in the receiver fluid of the Franz cells, which suggested that it could not pass through the silicone membrane.

**Cellulose ester membrane permeation.** A second artificial membrane study was performed using a porous membrane RCM to understand the diffusion of the  $\alpha$ -T esters without the process of membrane partitioning. The transport of  $\alpha$ -TP at pH 9 through the cellulose ester membrane was faster compared to pH 7.4 for each of the three different MWCO membranes (see Fig S4, Table 2) (0.5- 1 kDa-  $p < 0.01$ , Mann-Whitney nonparametric test, 20 kDa-  $p < 0.001$ , 1000 kDa-  $p < 0.001$ , Student's independent t-test). The 1000 kDa MWCO allowed the fastest permeation and the best reproducibility whereas the 0.5-1 kDa MWCO did not allow the  $\alpha$ -TP to permeate at pH 7.4.

Table 2: Flux at steady state from a 90% saturated solution  $\alpha$ -TP at pH 7.4 and 9 across three cellulose ester membranes. b) The change in flux upon increasing the pH was statistically significant for the cellulose ester membranes (0.5- 1 kDa-  $p$ -value  $< 0.01$ , Mann-Whitney's test, 20 kDa-  $p$ -value  $< 0.001$ , 1000 kDa-  $p$ -value  $< 0.001$ , Student's independent t-test). Data represent the mean  $\pm$  SD (n=5).

<b>Formulation</b>	<b>Cellulose ester membrane MWCO (KD) flux (µg/cm<sup>2</sup>/h)</b>		
	<b>0.5 – 1 kDa</b>	<b>20 kDa</b>	<b>1000 kDa</b>
<b><math>\alpha</math>-TP at pH 7.4</b>	Not detected	$6.20 \pm 7.50$	$329.19 \pm 62.44$
<b><math>\alpha</math>-TP at pH 9</b>	$8.80 \pm 13.74$	$37.27 \pm 1.16$	$1577.98 \pm 327.72$
<b><math>p</math>-value</b>	$p < 0.01$	$p < 0.001$	$p < 0.001$

**Skin deposition studies.** The effect of adding the phosphate onto the  $\alpha$ -T on the passage of the compounds into the different layers of the skin and through the skin was characterised using a skin deposition study with full mass balance recovery. At the 3 h time point, there was no active detected in the receiver fluid of the cells suggesting that there was no transdermal penetration. For  $\alpha$ -TP at pH 7.4 92% of the applied formulation remained on the skin surface, 3.8% deposited in the SC, 1.2% deposited in the epidermis and 0.34% deposited in the dermis (Fig 5). The amounts of  $\alpha$ -TP deposited in the SC and the epidermis was significantly higher compared to  $\alpha$ -T ( $505.98 \pm 295.93 \mu\text{g}$  vs  $41.46 \pm 3.97 \mu\text{g}$ ,  $p < 0.05$  and  $170.10 \pm 28.67 \mu\text{g}$  vs  $26.87 \pm 3.09 \mu\text{g}$ ,  $p < 0.001$ , *post hoc* Tukey's test, one-way ANOVA, respectively). The deposition of  $\alpha$ -TP at pH 7.4 and the  $\alpha$ -T in the dermis were not statistically different. The  $\alpha$ -TP deposition was comparable in the epidermis and dermis when administered using a pH 7.4 (aggregated form) and a pH 9 (non-aggregated form), but both formulations (pH 7.4 and 9) showed a higher deposition in the epidermis compared to the  $\alpha$ -TP commercial lotion formulation (pH=6.8) ( $p < 0.001$ , *post hoc* Tukey's test, one-way ANOVA) (Fig 5).  $\alpha$ -TP at pH 7.4 showed higher deposition in SC than pH 9 and the commercial formulations (Fig 5,  $p < 0.05$ , *post hoc* Tukey's test, one-way ANOVA). The high deposition of the  $\alpha$ -TP in the SC suggested that the aggregates were fusing with the SC layer.

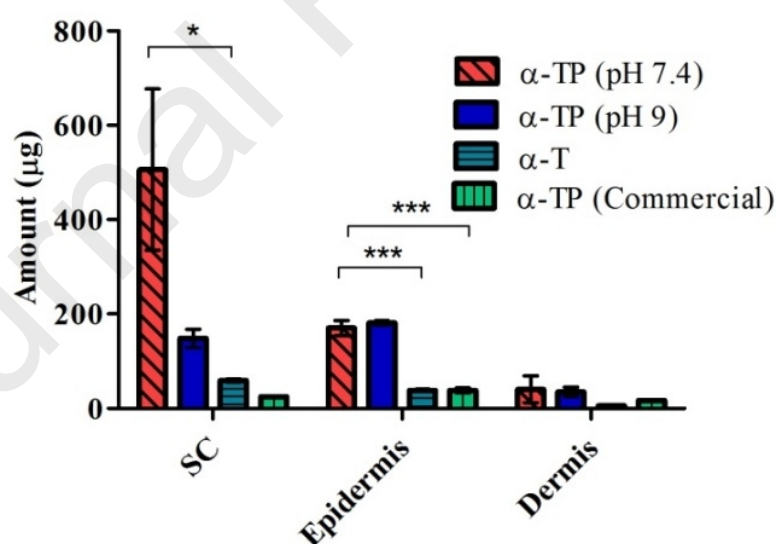


Fig. 5: Full-thickness porcine skin deposition 3 h after topically applying a dose of  $7.5 \text{ mg/cm}^2$  of active from each tested formulation. Both pH 7.4 and 9 of  $\alpha$ -TP lotions showed higher epidermal deposition compared to  $\alpha$ -T and the commercial  $\alpha$ -TP lotion (pH 6.8) ( $p < 0.001$ ). Data represent the mean  $\pm$  SD ( $n=3$ ).

**Monolayer subphase injection studies.** The interaction of the  $\alpha$ -T and  $\alpha$ -T esters with a model of the skin SC was investigated using monolayer subphase injection studies. The injection of  $\alpha$ -TP in the subphase of SC lipid monolayer, induced a surface pressure change of  $\sim 10$  mN/m whereas,  $\alpha$ -T and  $\alpha$ -TA induced a surface pressure change of less than 3 mN/m (Fig. 6). These small surface pressure changes for  $\alpha$ -T and  $\alpha$ -TA may be a consequence of low solubility in the subphase.  $\alpha$ -TA precipitated after injection and therefore less of the compound presumably interacted with the monolayer interface. The injection of an increased concentration of  $\alpha$ -TP (1, 2, and 12 mM) in the subphase led to a significant increase in the maximum obtained surface pressure compared to the vehicle control (1 mM-  $p < 0.001$ , 2 mM-  $p < 0.01$ , 12 mM-  $p < 0.01$ , One-way ANOVA with Dunnett's multiple comparisons test) (see Fig. 6, Table S3). The time to reach 50% of maximum surface pressure decreased significantly (1 mM-  $p = 0.001$ , 2 mM-  $p = 0.001$ , 12 mM-  $p < 0.001$ , One-way ANOVA with Dunnett's multiple comparisons test) for all the three concentrations compared to the vehicle control. The Hill slope significantly increased only for the injection of the 12.6 mM of  $\alpha$ -TP ( $p < 0.01$ , One-way ANOVA with Dunnett's multiple comparisons test). This indicated that the interaction with SC lipids occurred faster at the highest  $\alpha$ -TP concentration. This highest concentration was the only concentration above the  $\alpha$ -TP CAC which indicated that the aggregates had stronger interactions with the SC when in the aggregated form compared to the monomeric form>

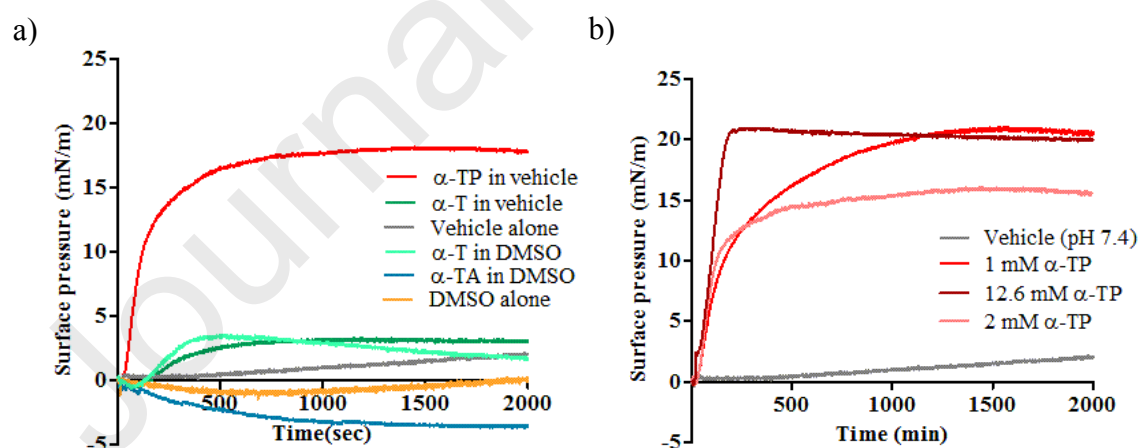


Fig. 6: The interaction kinetics following the injection into an SC lipid monolayer subphase. a)  $\alpha$ -TP vs  $\alpha$ -T in a 20:20:60 % (v/v/v) ethanol/propylene glycol/Tris buffer or DMSO b) The injection of an increasing concentration of  $\alpha$ -TP (1, 2, and 12 mM) in the vehicle 20:20:60 % (v/v/v) ethanol/propylene glycol/Tris buffer. Data represent the mean (n=3).

**Compression isotherm analysis.** The compression isotherm analysis was conducted to understand the interactions of the  $\alpha$ -TP esters once within the membrane structures as this helped to explain how the molecules may pass through the outer layer of the skin once it had partitioned into it. The data suggested that on their own, the SC lipids undergo a continuous phase transition from liquid expanded to liquid condensed phase. The monolayer lift-off value of pure SC lipids significantly increased with the addition of 30% of each of  $\alpha$ -TP,  $\alpha$ -T, and  $\alpha$ -TA ( $p < 0.05$ ,  $p < 0.01$ , and  $p < 0.05$ , respectively, One-way ANOVA with Dunnett's multiple comparisons test) (Fig. 7, Table S4). The shapes of the profiles suggested that  $\alpha$ -TP increased fluidity above 30%, but both  $\alpha$ -T, and  $\alpha$ -TA induced a first-order phase transition. The increased fluidity helped to explain why  $\alpha$ -TP seemed to show an easier transition from the SC into the epidermis compared to the other test agents.

The collapse pressure significantly decreased with the addition of 60%  $\alpha$ -TP, 30%  $\alpha$ -T, and 30%  $\alpha$ -TA ( $p < 0.05$ ,  $p < 0.01$ , and  $p < 0.01$ , respectively, One-way ANOVA with Dunnett's multiple comparisons test), which suggested that the additives dominated the membrane at high concentrations. The collapse area values were not statistically different upon the addition of all the three tocopherols to the SC lipid monolayer compared to the pure SC lipid monolayer ( $p > 0.05$ ).

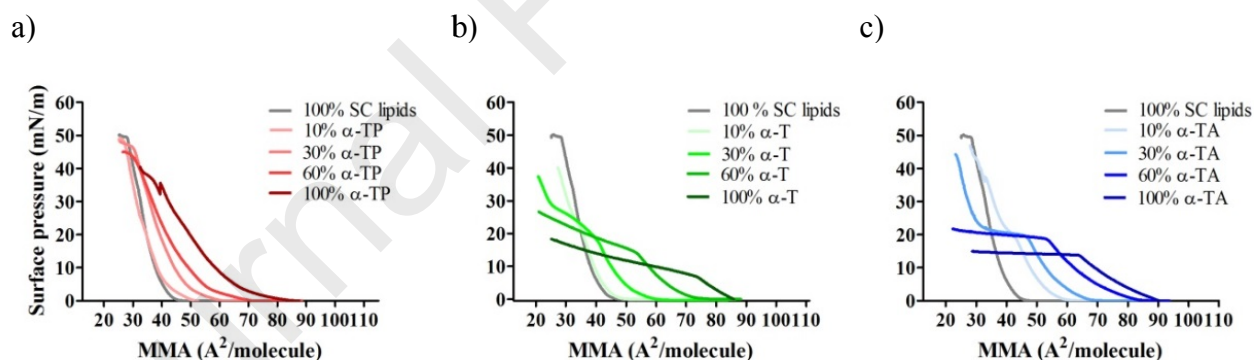


Fig. 7:  $\pi$ -A isotherms for interactions with the stratum corneum (SC) lipids (grey line) using  $\alpha$ -TP,  $\alpha$ -T, and  $\alpha$ -TA and their mixtures. a)  $\alpha$ -TP and  $\alpha$ -TP: SC lipid mixtures, b)  $\alpha$ -T and  $\alpha$ -T: SC lipid mixtures, c)  $\alpha$ -TA and  $\alpha$ -TA: SC lipid mixtures, at composition ratio of 10%, 30%, and 60% (v/v) at pH 7. Data represent mean  $\pm$  SD (n=3).

At all surface pressures (1-30 mN/m) the MMA of pure SC lipids increased with the addition of 30%  $\alpha$ -TP ( $p < 0.05$ , unpaired Student t-test) (Fig. 8a). For instance, at surface pressure 30 mN/m, the MMA of SC lipids ( $30.18 \pm 4.75 \text{ Å}^2$ ) increased with the addition of 30%  $\alpha$ -TP up to  $38.12 \pm 3.61 \text{ Å}^2$  ( $p < 0.05$ , One-way ANOVA with Dunnett's multiple comparisons test).

This was thought to be due to an increase of the repulsive forces and the steric hindrance upon increasing the percentage of  $\alpha$ -TP in the monolayer, which weakened the attraction forces between SC lipid hydrophilic head groups and fluidized the monolayer. The addition of 30%  $\alpha$ -T increased the MMA of pure lipids at 1-20 mN/m (1-5 mN/m –  $p < 0.01$ , 10-15 mN/m –  $p < 0.05$ , One-way ANOVA with Dunnett's multiple comparisons test, 20 mN/m,  $p = 0.05$ , One-way ANOVA with Games-Howell test), but there was no significant increase at higher surface pressures (25-30 mN/m –  $p > 0.05$ , One-way ANOVA with Games-Howell's test) (Fig. 8b). The 60%  $\alpha$ -TA increased the MMA of pure lipids at 1-20 mN/m (1-5 mN/m –  $p < 0.0001$ , 10-15 mN/m –  $p < 0.01$ , One-way ANOVA with Dunnett's multiple comparisons test), but there was no significant increase at 20-25 mN/m ( $p > 0.05$ , One-way ANOVA with Games-Howell's test) (Fig. 8c).

In this study, the SC lipids/ $\alpha$ -TP mixtures were not ideally mixed in all compositions studied (Fig. 8a). Their MMAs were higher than those calculated from the equation of additivity rule at each surface pressure except for the addition of 10%  $\alpha$ -TP, which indicates stronger repulsive or weaker attractive interactions between SC lipids and  $\alpha$ -TP compared to the SC lipids/SC lipids and  $\alpha$ -TP/ $\alpha$ -TP interaction. In the equimolar Cer/Chol/PA SC lipid model  $\alpha$ -TP becomes the most abundant single component at a molar concentration above 25%. This emphasizes that at 30%  $\alpha$ -TP, i.e., when  $\alpha$ -TP dominates the composition of the mixture, an inflection point was observed in the MMA curve. This may be a consequence of changing the interactions between  $\alpha$ -TP and SC lipids as the concentration of  $\alpha$ -TP increases and becomes the dominant species in the monolayer, which switches from the ordered rigid SC lipids to the more liquid expanded films. The repulsive interactions between the SC lipids and  $\alpha$ -T or  $\alpha$ -TA were to a lesser degree or absent at surface pressure  $> 15$  mN/m (Figs. 8b, c).

The surface compressional moduli were determined from the  $\Pi$ -A isotherms to determine the effect of increasing the  $\alpha$ -TP concentration on the elasticity of SC lipid monolayers. This parameter was calculated from the tangent of the isotherms at 10, 20, 30, and 40 mN/m using eq 4. Table S5 shows that at 30 mN/m, there is an overall trend to decrease of the calculated surface compressional moduli for the SC lipid monolayers as the  $\alpha$ -TP concentration increases above a 10% molar percentage (30% and 60% w/w compared to pure SC control sample, 30% –  $p < 0.001$  and 60% –  $p < 0.0001$ , One-way ANOVA with Dunnett's multiple comparisons test), at 30%  $\alpha$ -TP the magnitude of these changes is comparatively small, as the  $K^s$  values for

all of the monolayers fall within the liquid condensed phase (100- 250 mN/m), whereas the magnitude of change was higher at 60%  $\alpha$ -TP, the  $K^s$  value was below 100 mN/m indicates an intermediate phase between liquid expanded and liquid condensed (50-100 mN/m).

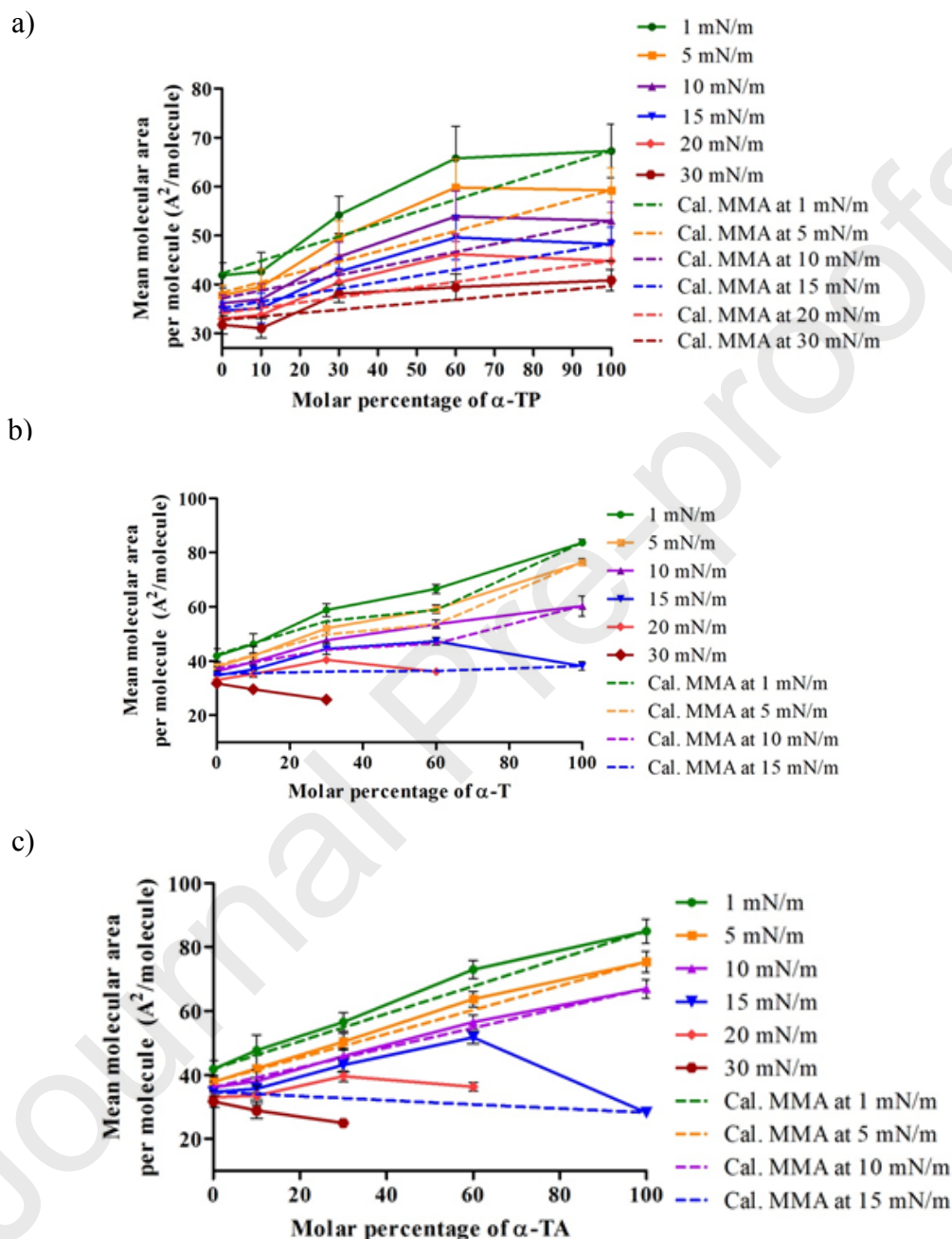


Fig. 8: Mean molecular area for Cer/Chol/PA and  $\alpha$ -TP (a),  $\alpha$ -T (b), and  $\alpha$ -TA (c) mixtures at a surface pressure of 1, 5, 10, 15, 20, and 30 mN/m. The solid lines represent the measured MMA from the isotherms, and the dashed lines are the calculated ideal mixing curves. At surface pressure 30 mN/m, the addition of 30%  $\alpha$ -TP mixture increased the measure MMA of SC lipid at the inflection point whereas the addition of 30%  $\alpha$ -T or  $\alpha$ -TA did not.



There was a general decrease in the calculated surface compressional moduli for the SC lipid monolayers as the  $\alpha$ -T concentration increased (10-30 % w/w compared to SC only control sample, 10% -  $p < 0.05$ , 30% -  $p < 0.0001$ , One-way ANOVA with Games-Howell's test, see, Table S6). The magnitude of these changes was relatively small, as the  $K^s$  values for of 10%  $\alpha$ -T the  $K^s$  value was below 100 mN/m indicates an intermediate phase between LE and LC (50-100 mN/m), whereas at 30% monolayers the magnitude of change is higher i.e. shift from the liquid condensed (LC) phase to liquid expanded (LE) (12.5-50 mN/m). The increased concentration of  $\alpha$ -TA percentage (10-30%) also showed a significant decrease in the  $K^s$  ( $p < 0.0001$ , One-way ANOVA with Dunnett's multiple comparisons test) (Table 7). However, the magnitude of these changes at 10% for  $\alpha$ -TA was low, as the  $K^s$  values for the monolayer fall within the liquid condensed (LC) phase, whereas at a 30% intermediate phase between LE and LC (100- 250 mN/m). The monolayer collapse pressure decreased significantly upon increasing the molar percentage of the monolayer of  $\alpha$ -T or  $\alpha$ -TA, making the  $K^s$  calculation impossible for higher surface pressure e.g. at 30 mN/m at a molar percentage of 60%.

## Discussion

$\alpha$ -TP was used in this study in its phosphate disodium salt form, but it was assumed that this amphiphilic molecule would rapidly dissociate in water to produce either the non-ionic, monoionic, or dianionic forms, depending on the pH. The solubility of  $\alpha$ -TP increased in the ethanol/propylene glycol/Tris 20:20:60 % v/v/v co-solvent vehicle as the pH increased and this was most notable when the pH was higher than the  $pK_{a2}$  of  $\alpha$ -TP. These data indicated that the percentage of  $\alpha$ -TP in the di-anionic form was critical to its aqueous solubility. The lower aqueous solubility of  $\alpha$ -TP at pH 7.4 was thought to be responsible for its aggregation at this pH in the co-solvent vehicle. The CAC at pH 7.4 was in the millimolar concentration range, which was similar to the prodrug dexamethasone phosphate (15), but when the pH, hence the  $\alpha$ -TP solubility, increased to pH 9 no aggregation was observed. The aggregate analysis using both DLS and AFM indicated that the  $\alpha$ -TP aggregates were smaller than the  $\alpha$ -T aggregates, although it was noted that this comparison was weakened by unavoidable concentration differences in the measured samples. There were discrepancies observed in the size of the aggregates obtained using the AFM and the DLS, which may have been due to the drying process on the mica surface, but the trends in the two data sets were consistent. The  $\alpha$ -TP aggregates appeared to be similar to the unilamellar vesicles described in the literature at pH



7.4 in previous work (28,29), but further evidence, which was not collected in this study, was required to confirm the aggregate structure. The aggregate shape was influenced by concentration, but at a given concentration the  $\alpha$ -TP aggregates were physically stable over 7 days.

The degradation of  $\alpha$ -TP at 100  $\mu\text{g/mL}$  in the ethanol/propylene glycol/Tris HCl 20:20:60 % v/v/v co-solvent using the 'fit-for-purpose' HPLC assay proceeded at a rate of 2.26  $\mu\text{g/mL/week}$  (i.e., 2.3%/week). This demonstrated that  $\alpha$ -TP was more stable than  $\alpha$ -T which had previously been shown to degrade at 25% per week, a rate that is not suitable for cosmetic products (20,30).

The model membrane transport data showed that  $\alpha$ -TP aggregation slowed down the diffusion of the  $\alpha$ -TP molecules. However, the *ex-vivo* skin permeation studies demonstrated that the amount of  $\alpha$ -TP deposited in the skin was comparable using both the aggregated and non-aggregated  $\alpha$ -TP preparations. The synthetic regenerated cellulose membrane studies measured the effects of aggregation on the self-diffusion, i.e., the diffusion through the vehicle in the aggregated and non-aggregated forms because no partitioning into the porous regenerated membrane was expected. Although the skin deposition data would also be subject to the same change in self-diffusion caused by aggregation, it may have been masked by the more complex permeation process in human skin, which allowed the potential for follicular transport and fusion of the aggregates with the SC. The fact that  $\alpha$ -TP aggregates showed superior SC (12.2-fold) and epidermal (6.3-fold) deposition compared to  $\alpha$ -T suggested that  $\alpha$ -TP showed a different affinity for the SC and the more hydrophilic layers of skin underlying the SC when it penetrated the tissue. As the enhancement in SC deposition was only observed when the aggregates were used it suggested that the aggregates fused with the SC. Comparison of the  $\alpha$ -TP to other pro-drugs of  $\alpha$ -T such as  $\alpha$ -TA, alanine, glycine, and pyroglutamic acid conjugates, and tocopherol glycoside indicates that  $\alpha$ -TP was superior in terms of epidermal deposition (31,32).

The aqueous monolayers of equimolar mixtures of ceramide, cholesterol, and PA were used to mimic a single layer of intercellular SC lipid lamellae.  $\alpha$ -TP demonstrated a stronger and faster interaction with the lipid monolayer than  $\alpha$ -T in the monolayer subphase injection studies. This indicated that the surfactant properties of  $\alpha$ -TP allowed insertion into hydrophobic regions of SC lipid film, whereas  $\alpha$ -T did not (33). Overtime  $\alpha$ -T formed an oily second phase because of

its lack of  $\alpha$ -T-SC lipid interactions, but the oil did not sediment and hence it was not thought to interfere with the measurements. When  $\alpha$ -TP was presented to the monolayer as an aggregate its interaction was faster compared to the unaggregated form at the same pH and this supported the notion that in the aggregated form the  $\alpha$ -TP fused with the SC lipids.

The Langmuir  $\Pi$ -A isotherms for the SC lipids lift-off ( $45.38 \pm 5.51 \text{ \AA}^2$ ) and collapse ( $26.58 \pm 4.04 \text{ \AA}^2$ ) and collapse pressure ( $48.82 \pm 2.21 \text{ mN/m}$ ) were in good agreement with the literature (19,34). These values indicated that SC lipids formed rigid, condensed monolayers in the air/aqueous interface model. All the pure films suggested a liquid-expanded state, but the data when  $\alpha$ -T and  $\alpha$ -TA were added to the films suggested that they may be more tilted towards the interface compared to  $\alpha$ -TP. The transition of the  $\Pi$ -A isotherms of pure films were not due to any change in the phase-state of the  $\alpha$ -T and TA at the air/buffer interface, and they did not show the presence of the liquid-condensed phase, as evidenced by the values of the compressibility modulus ( $k^s < 50 \text{ mN/m}$ ) (13.6 and 45.9 mN/m, respectively, at surface pressure 10 mN/m) (24,26,35).

The MMA of pure SC lipids (at surface pressure 30 mN/m) significantly increased with the addition of 30%  $\alpha$ -TP, due to an increase in the repulsive forces and the steric hindrance upon addition of  $\alpha$ -TP. The consequence of this was weaker attractive forces or stronger repulsive between SC lipid hydrophilic head groups with the  $\alpha$ -TP fluidizing the monolayer as a result. It has been reported in the literature that  $\alpha$ -TP fluidizes membranes and induces hemolysis in a concentration-dependent manner, i.e., it can act as a detergent (36). This fluidisation explains why the  $\alpha$ -TP could pass beyond the SC and into the epidermis. The addition of 30%  $\alpha$ -T or  $\alpha$ -TA did not change the MMA of the pure lipids. This indicated that these molecules were likely to separate from the SC lipid monolayer, i.e., there was a weaker interaction and poorer mixing between the SC lipids and either  $\alpha$ -T or  $\alpha$ -TA, compared to  $\alpha$ -TP. This data supported the notion that  $\alpha$ -T and  $\alpha$ -TA found it difficult to enter the SC monolayer. The measured MMA of the SC- $\alpha$ -TP mixtures were higher than the calculated values, but previous work with oleic acid, a known skin penetration enhancer, found that the measured MMA of SC lipid-OA mixtures were significantly lower than the calculated MMA at each surface pressure. These differences suggested that the interactions of  $\alpha$ -TP could fluidise the SC, but it did not disrupt the SC like oleic acid (19,29).

A lower compressibility modulus ( $K^s$ ) indicates a monolayer with lower interfacial stiffness and thus higher elasticity. SC lipids at 30 mN/m displayed a compressibility modulus  $K^s$  up to  $169.44 \pm 11.67$  mN/m. The addition of 60%  $\alpha$ -TP significantly reduced the compressibility modulus  $K^s$ , which provided further evidence that  $\alpha$ -TP fused with, and integrated into the SC lipids to change their properties from liquid condensed into the more liquid expanded film, i.e., disturbed the lipid packing and fluidized the membrane.  $\alpha$ -T or TA could not adopt a liquid condensed state, i.e., they could not be compressed at high surface pressure. This meant that both controls could not be packed easily as  $\alpha$ -TP into the membrane. The amphiphilic balance present in  $\alpha$ -TP seemed to allow it to adopt a perpendicular orientation to form a stable monolayer at the interphase, mix well with the SC lipid monolayer, and to move or diffuse through lipids. However,  $\alpha$ -T and  $\alpha$ -TA, which lacked the amphiphilic balance, probably display a parallel (flat) orientation at the SC interface and remained phase separated. This helps to explain why in this study, and previously published work,  $\alpha$ -T finds it difficult to pass through the skin (37). The plateau observed in the compression isotherm of the pure  $\alpha$ -T and  $\alpha$ -TA monolayers was similar to that of a pure fengycin monolayer, reported in a study by Eeman *et al.* In this previous work, the fengycin was squeezed out of the mixed monolayers when the monolayer pressure was increased and thus it was unable to diffuse through extracellular lipid matrix of SC model (38).

## Conclusion

This study demonstrated that the phosphate ester of  $\alpha$ -T was able to penetrate more efficiently into the viable epidermis of the skin despite its propensity to self-associate in polar delivery vehicles. The high SC deposition of the  $\alpha$ -TP when it formed aggregates suggested that it was the aggregation process, which drove the propensity of the  $\alpha$ -TP to fuse with the SC layer. The lipid monolayer studies supported the notion that the  $\alpha$ -TP aggregates more readily interacted with the SC compared to both  $\alpha$ -T and  $\alpha$ -TP monomers. It appeared that the structural similarity of  $\alpha$ -TP to the phospholipids allowed it to approach and partition into SC lipid monolayer and fluidize it. The presence of  $\alpha$ -TP in the SC lipid monolayer was better tolerated than  $\alpha$ -T because  $\alpha$ -TP could change its orientation to suit the lipid packing. This helps to explain why  $\alpha$ -T/ $\alpha$ -TA, which were lodged in the lipid bilayer, and hardly passed through the lipids, had difficulty in penetrating the skin epidermis whereas  $\alpha$ -TP, which was more mobile and more readily moved through the lipid matrix, could access the epidermis. It was notable that although

$\alpha$ -TP displayed a charged head group, it could still pass the lipid lamellae in the skin and permeate the skin presumably through the intercellular route. However, the silicone membrane, suggested that  $\alpha$ -TP would not pass through the skin. The silicone membrane does provide a hydrophobic barrier, but it lacks the lipid domains/lamellae and charged molecules displayed in the skin, which undoubtedly affect the permeation process in real tissue. These Langmuir penetration kinetics and compression isotherm results suggested  $\alpha$ -TP nanoaggregates are likely to be transported through intercellular SC lipid matrix possibly by fusion with SC lipids to reach the viable epidermis where it can act as an antioxidant and may protect from UVR-induced skin damage.

## Supporting information

The supporting information is available online.

## Funding Information

The University of Jordan provided funding for MS.

## References

- [1] S. Farahmand and H.I Maibach, Transdermal drug pharmaco-kinetics in man: Inter-individual variability and partial prediction, *Int J Pharm*, 367 (2008) 1–15.
- [2] E. Jungman. Development of a percutaneous penetration predictive model with chromatographic and spectroscopic tools, PhD thesis, Université Paris Sud - Paris XI, 2012.
- [3] S. Wiedersberg, R. H. Guy, Transdermal Drug Delivery: 30+ Years of War and Still Fighting! *J. Control. Release*. 190 (2014) 150-156.
- [4] A. S Michaels, S. K. Chandrasekaran, J. E. Shaw, Drug Permeation through Human Skin: Theory and Invitro Experimental Measurement, *AIChE J.* 21 (1975) 985–996.
- [5] P. M. Elias, E. R. Cooper, A. Korc, B. E. Brown, Percutaneous Transport in Relation to Stratum Corneum Structure and Lipid Composition, *J. Invest. Dermatol.* 76 (1981) 297–301.
- [6] Z. Nemes, P. M. Steinert, Bricks and Mortar of the Epidermal Barrier. *Exp. Mol. Med.* 31 (1999) 5.
- [7] S. Premi, S. Wallisch, C. M. Mano, A. B. Weiner, A. Bacchiocchi, K. Wakamatsu, E. J.

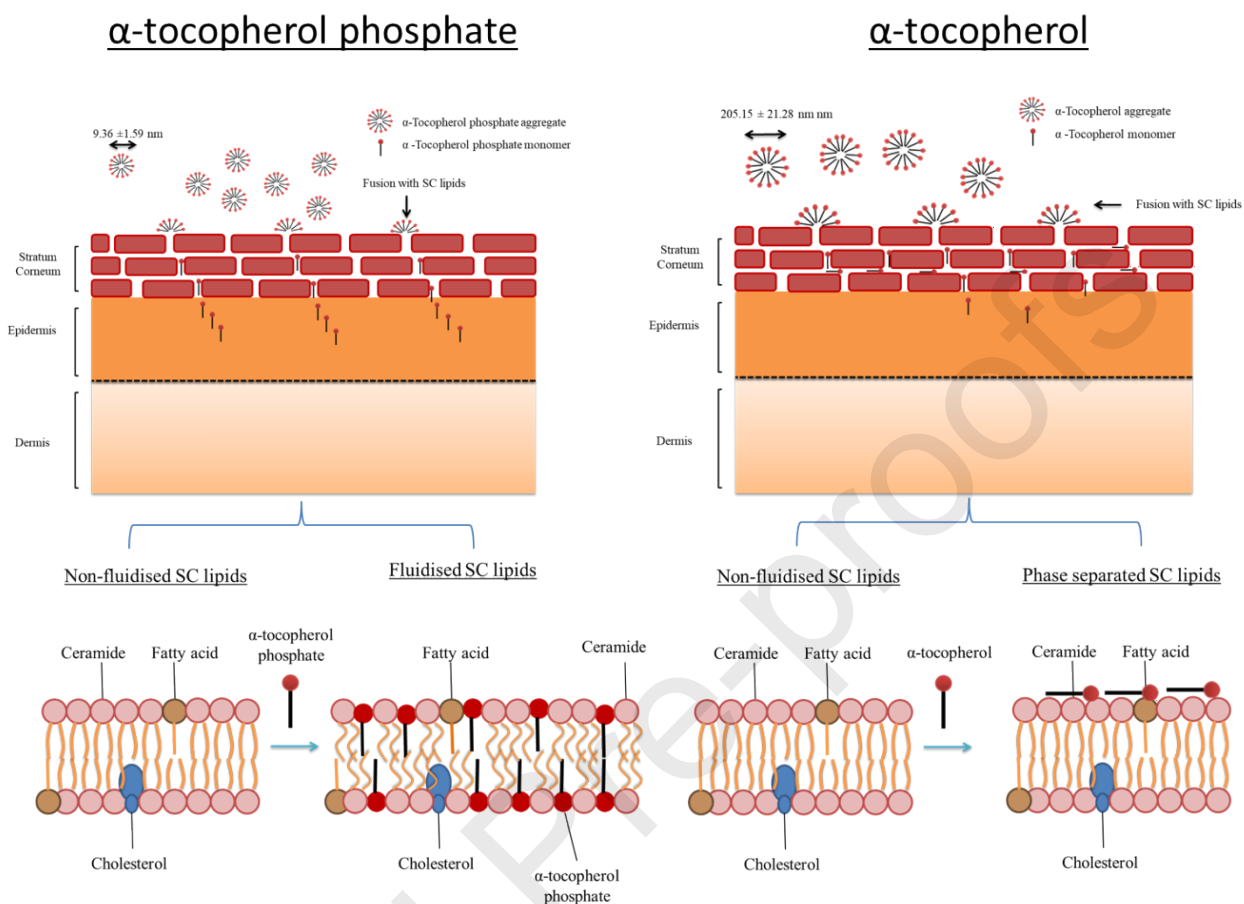
- H. Bechara, R. Halaban, T. Douki, D. E. Brash, Chemiexcitation of Melanin Derivatives Induces DNA Photoproducts Long after UV Exposure, *Science*. 347 (2015) 842–847.
- [8] T. Douki, A. Reynaud-Angelin, J. Cadet, E. Sage, Bipyrimidine Photoproducts Rather than Oxidative Lesions Are the Main Type of DNA Damage Involved in the Genotoxic Effect of Solar UVA Radiation. *Biochemistry* 42 (2003) 9221–9226;
- [9] G. J. Delinasios, M. Karbaschi, M. S. Cooke, A. R. Young, Vitamin E Inhibits the UVAI Induction of “Light” and “Dark” Cyclobutane Pyrimidine Dimers, and Oxidatively Generated DNA Damage, in Keratinocytes. *Sci. Rep.* 8 (2018) 423.
- [10] A. Cichewicz, C. Pacleb, A. Connors, M. A. Hass, L. B. Lopes, Cutaneous Delivery of Alpha-Tocopherol and Lipoic Acid Using Microemulsions: Influence of Composition and Charge. *J. Pharm. Pharmacol.* 65 (2013) 817–826.
- [11] S. Nakayama, E. M. Katoh, T. Tsuzuki, S. Kobayashi, Protective Effect of Alpha-Tocopherol-6-O-Phosphate against Ultraviolet B-Induced Damage in Cultured Mouse Skin. *J. Invest. Dermatol.* 121 (2003) 406–411.
- [12] X. J Cai, T. Patel, A. Woods, P. Mesquida, S.A. Jones, Investigating the Influence of Drug Aggregation on the Percutaneous Penetration Rate of Tetracaine When Applying Low Doses of the Agent Topically to the Skin. *Int. J. Pharm.* 502 (2016) 10–17.
- [13] R. Inacio, D. Barlow, X. Kong, J. Keeble, S. A. Jones. Investigating How the Attributes of Self-Associated Drug Complexes Influence the Passive Transport of Molecules through Biological Membranes. *Eur. J. Pharm. Biopharm.* 102 (2016) 214–222.
- [14] B. M. Rezk, G. R. M. Haenen, W. J. van der Vijgh, A. Bast. The Extraordinary Antioxidant Activity of Vitamin E Phosphate. *Biochim. Biophys. Acta - Mol. Cell Biol. Lipids*. 1683 (2004) 16–21.
- [15] A. Shah, A. M. Khan, M. Usman, R. Qureshi, M. Siddiq, S. S. Shah, Thermodynamic Characterization of Dexamethasone Sodium Phosphate and Its Complex with DNA as Studied by Conductometric and Spectroscopic Techniques. *J. Chil. Chem. Soc.* 54 (2009) 134–137.
- [16] E. Kato, Y. Sasaki, N. Takahashi, Sodium DL-Alpha-Tocopheryl-6-O-Phosphate Inhibits PGE(2) Production in Keratinocytes Induced by UVB, IL-1 $\beta$  and Peroxidants. *Bioorg. Med. Chem.* 19 (2011) 6348–6355.
- [17] E. Abd, S. A. Yousef, M. N. Pastore, K. Telaprolu, Y.H. Mohammed, S. Namjoshi, J. E. Grice, M. S. Roberts, Skin Models for the Testing of Transdermal Drugs. *Clin. Pharmacol.* 8 (2016) 163–176.
- [18] A. M. Barbero, H. F. Frasch, Pig and Guinea Pig Skin as Surrogates for Human in Vitro Penetration Studies: A Quantitative Review. *Toxicol. Vitro*. 23 (2009) 1–13.
- [19] G. Mao, D. VanWyck, X. Xiao, M. C. Mack Correa, E. Gunn, C. R. Flach, R. Mendelsohn, R. M. Walters, Oleic Acid Disorders Stratum Corneum Lipids in Langmuir

- Monolayers. *Langmuir*. 29 (2013) 4857–4865.
- [20] R. A. Harper, M. M. Saleh, G. Carpenter, V. Abbate, G. Proctor, R. D. Harvey, R. J. Gambogi, A. Geonnotti, R. Hider, S. A. Jones. Soft, Adhesive (+) Alpha Tocopherol Phosphate Planar Bilayers That Control Oral Biofilm Growth through a Substantive Antimicrobial Effect. *Nanomedicine*. 14 (2018) 2307-2316.
  - [21] F. L. Primo, M. M. A. Rodrigues, A. R. Simioni, M. V. L. Bentley, P. C. Morais, A. C. Tedesco, In Vitro Studies of Cutaneous Retention of Magnetic Nanoemulsion Loaded with Zinc Phthalocyanine for Synergic Use in Skin Cancer Treatment. *J. Magn. Magn. Mater.* 320 (2008) e211–e214.
  - [22] N. V. Sheth, M. B. McKeough, S. L. Spruance, Measurement of the Stratum Corneum Drug Reservoir to Predict the Therapeutic Efficacy of Topical Iododeoxyuridine for Herpes Simplex Virus Infection. *J. Invest. Dermatol.* 89 (1987) 598–602.
  - [23] W. Diembeck, H. Beck, F. Benech-Kieffer, P. Courtellemont, J. Dupuis, W. Lovell, M. Paye, J. Spengler, W. Steiling, Test Guidelines for in Vitro Assessment of Dermal Absorption and Percutaneous Penetration of Cosmetic Ingredients. *European Cosmetic, Toiletry and Perfumery Association. Food Chem. Toxicol.* 37 (1999) 191–205.
  - [24] R. Maget-Dana, The Monolayer Technique: A Potent Tool for Studying the Interfacial Properties of Antimicrobial and Membrane-Lytic Peptides and Their Interactions with Lipid Membranes. *Biochim. Biophys. Acta* 1463 (1999) 109–140.
  - [25] M. A. Alsina, A. Ortiz, D. Polo, F. Comelles, F. Reig, Synthesis and Study of Molecular Interactions between Phosphatidyl Choline and Two Laminin Derived Peptides Hydrophobically Modified. *J. Colloid Interface Sci.* 294 (2006) 385–390.
  - [26] J. T. Davies, E. K. Rideal, *Interfacial Phenomena*, Academic Press, New York. 1981.
  - [27] S. R. Dennison, F. Harris, D. A. A. Phoenix, *Langmuir Approach Using on Monolayer Interactions to Investigate Surface Active Peptides*. *Protein Pept. Lett.* 17 (2010) 1363–1375.
  - [28] M. S. Muthu, S. Avinash Kulkarni, Y. Liu, S. S. Feng, Development of Docetaxel-Loaded Vitamin E TPGS Micelles: Formulation Optimization, Effects on Brain Cancer Cells and Biodistribution in Rats. *Nanomedicine*. 7 (2012) 353–364.
  - [29] P. D. Gavin, M. El-Tamimy, H. H. Keah, B. J. Boyd, Tocopheryl Phosphate Mixture (TPM) as a Novel Lipid-Based Transdermal Drug Delivery Carrier: Formulation and Evaluation. *Drug Deliv. Transl. Res.* 7 (2017) 53–65.
  - [30] P. Stephane, Stability of Cosmetic Formulations Containing UV Filters and Preservatives, Based on Physical and Chemical Parameters. *MOJ Toxicol.* 1 (2015)12–21.
  - [31] C. Ostacolo, F. Marra, S. Laneri, A. Sacchi, S. Nicoli, C. Padula, P. Santi, Alpha-Tocopherol pro-Vitamins: Synthesis, Hydrolysis and Accumulation in Rabbit Ear Skin.

- J. Control. Release. 99 (2004) 403–413.
- [32] A. Mavon, V. Raufast, D. Redoules. Skin Absorption and Metabolism of a New Vitamin E Prodrug, Delta-Tocopherol-Glucoside: In Vitro Evaluation in Human Skin Models. J Control. Release. 100 (2004) 221–231.
- [33] P. Nigam, Interaction of Water-Soluble Surfactants with Self-Assembled Lipid Monolayers at the Vapor-Liquid Interface: Equilibrium and Dynamic Phenomena PhD Thesis, The Ohio State University, 2006.
- [34] C. R. Flach, R. Mendelsohn, M. E. Rerek, D. J. Moore, Biophysical Studies of Model Stratum Corneum Lipid Monolayers by Infrared Reflection–Absorption Spectroscopy and Brewster Angle Microscopy. J. Phys. Chem. B. 104 (2000) 2159–2165.
- [35] M. Elderdfi, A. F. Sikorski. Langmuir-Monolayer Methodologies for Characterizing Protein-Lipid Interactions, Chem. Phys. Lipids. 212 (2018) 61–72.
- [36] B. M. Rezk, W. J. van der Vijgh, A. Bast, G. R. Haenen. Alpha-Tocopheryl Phosphate Is a Novel Apoptotic Agent, Front. Biosci. 12 (2007) 2013–2019.
- [37] Gabbanini S, Matera R, Beltramini C, Minghetti A, Valgimigli L. Analysis of in vitro release through reconstructed human epidermis and synthetic membranes of multi-vitamins from cosmetic formulations. J Pharm Biomed Anal. 2010 Aug 1;52(4):461-7.
- [38] M. Eeman, G. Francius, Y. F. Dufrêne, K. Nott, M. Paquot, M. Deleu, Effect of Cholesterol and Fatty Acids on the Molecular Interactions of Fengycin with *Stratum Corneum* Mimicking Lipid Monolayers, Langmuir. 25 (2009) 3029–3039.



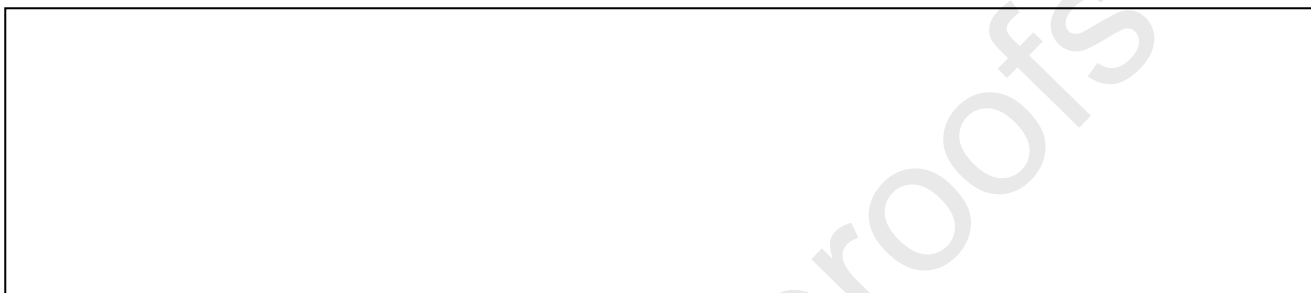
## Graphical Abstract



**Declaration of interests**

☒ The authors declare that they have no known competing financial interests or personal relationships that could have appeared to influence the work reported in this paper.

☐ The authors declare the following financial interests/personal relationships which may be considered as potential competing interests:

**Nanomaterials fusing with the skin: alpha-tocopherol phosphate delivery into the viable epidermis to protect against ultraviolet radiation damage**

Mais M. Saleh Investigation, Writing- Original draft preparation. Arcadia Woods. Methodology. Richard D. Harvey Supervision, Methodology, Reviewing and Editing Antony R. Young Supervision, Reviewing and Editing Stuart A. Jones Conceptualization, Writing- Original draft preparation, supervision, reviewing and editing.